Advanced and Sustainable Technologies
ASET
E-ISSN 2976-2294

Volume 5, No 2, September 2026 [10-26]

Finite Element Analysis on Shear Strengthened Reinforced Concrete Beam with Different Orientations of Carbon Fibre Reinforced Polymer (CFRP)

Rishitaran Pannir Selvam[1], N A Hashim[1,2]* and H N Yakin[3]

[1]Faculty of Civil Engineering & Technology, Kompleks Pusat Pengajian Jejawi 3, Universiti Malaysia Perlis, 02600 Arau, Perlis, Malaysia.
[2]Sustainable Environment Research Group (SERG), Centre of Excellence Geopolymer and Green Technologies (CEGeoGTech), Universiti Malaysia Perlis, Kompleks Pengajian Jejawi 2, 02600 Arau, Perlis, Malaysia.
[3]Faculty of Civil Engineering, Universiti Teknologi Malaysia, 81310 Johor Bahru, Johor, Malaysia.

Received 11 February 2026, Revised 25 March 2026, Accepted 8 May 2026

ABSTRACT

Shear failure in reinforced concrete (RC) beams is a critical structural issue that can lead to sudden, catastrophic collapse. Carbon fibre reinforced polymer (CFRP) sheets have emerged as an effective retrofitting material due to their high strength-to-weight ratio, corrosion resistance, and ease of application. However, the influence of CFRP wrapping angles on shear performance remains insufficiently explored. This study investigates the impact of varying CFRP wrapping angles on the structural behaviour of RC beams to optimize shear strengthening. Using finite element analysis (FEA) in ABAQUS software, eight RC beam specimens with CFRP wrapping angles of 30°, 35°, 40°, 45°, 50°, 55°, 60°, and 90° were analysed under four-point bending. Key metrics, including shear capacity, stress distribution, and tensile stress, were evaluated. Results demonstrated that mid-range wrapping angles, particularly 35°, 40°, and 60°, significantly enhanced shear capacity and shifted failure modes from brittle to ductile, improving structural resilience. Detailed stress and deformation analyses revealed the mechanics of CFRP-strengthened beams, emphasizing the transformative impact of optimizing wrapping angle. This research addresses a critical gap in the literature and offers actionable insights to optimize CFRP retrofitting strategies. The findings contribute to enhancing the durability, safety, and sustainability of RC structures, offering a robust framework for modern structural rehabilitation (SDG 9) and sustainable construction practices (SDG 11).

Keywords: Carbon fiber reinforced polymer, Finite element analysis, Reinforced concrete, Shear failure.

1. INTRODUCTION

Reinforced concrete (RC) is a composite material, designed to combine the compressive strength of concrete with the tensile strength of steel [1] extensively utilized to resist external loads such as wind, vibrations, earthquakes, and all other sources of tensile and shear stresses, preventing the concrete from cracking, crumbling, or breaking completely. However, RC structures, particularly beams, the horizontal components of RC structures that carry and transfer lateral loads across other structural elements such as columns and walls [2], are susceptible to deterioration over time due to factors such as environmental exposure, overloading, and material

*Corresponding author: aniraasyikin@unimap.edu.my

degradation, leading to a reduction in shear capacity. This reduction in shear strength can severely compromise the structural integrity and safety of concrete elements [3]. To address these challenges, it is crucial to refine how we reinforce these beams, ensuring they can withstand modern loading demands while maintaining long-term performance. Among the most promising reinforcement methods, Fibre Reinforced Polymer (FRP) composites, particularly Carbon Fibre Reinforced Polymer (CFRP), have gained significant attention due to their exceptional mechanical properties, including high tensile strength, low weight, and corrosion resistance [4,5]. FRP systems consist of various fibres, including carbon, glass, aramid, and basalt, with CFRP being the most widely used for its superior strength-to-weight ratio and durability. The application of CFRP to RC beams can be implemented through techniques such as the externally bonded (EB) system and the near-surface mounted (NSM) system, both of which have been extensively studied [6,7]. Despite the widespread use of CFRP in strengthening RC structures, challenges persist in optimizing its application, particularly regarding the orientation of CFRP sheets and their impact on shear strength and overall structural performance.

The use of CFRP for shear strengthening of RC beams has been extensively studied, with various factors influencing its effectiveness. Studies by [5] and [6] have demonstrated that parameters such as CFRP fibre ratio, shear-span ratio, and concrete strength significantly impact the shear performance of RC beams. Mhanna et al. have also emphasized the importance of bonding techniques and the role of CFRP sheets in resisting shear forces [7]. While these studies have contributed to a deeper understanding of CFRP strengthening, a gap exists in the literature regarding the specific impact of CFRP wrapping angles on shear strength. Most studies have focused on CFRP use without considering the effects of varying wrapping angles, which could optimize the strengthening process. Furthermore, although the EB and NSM systems have been well documented, the influence of different CFRP orientations on shear capacity remains to be fully explored.

In this paper, the shear strengthening of RC beams using CFRP sheets at various orientations is investigated through Finite Element Analysis (FEA). The primary objective of this research is to explore the mechanical behaviour and shear capacity of 8 RC beams strengthened with CFRP sheets wrapped at different angles of 30°, 35°, 40°, 45°, 50°, 55°, 60°, and 90°. The approach involves conducting FEA simulations to assess the impact of CFRP wrapping angles on the shear strength and overall performance of the beams. Specifically, the study will focus on how CFRP sheet orientation influences the distribution of compressive stresses, tensile stress, and displacement in shear-strengthened RC beams. The methodology will involve rigorous FEA simulations to provide a detailed assessment of the shear-strengthening process and to inform the design and implementation of CFRP-based solutions to enhance the resilience of concrete structures.

2. MATERIAL AND METHODS

In this study, the preparation of the supported (pin and roller) rectangular reinforced concrete (RC) beam model measuring 3200 × 250 × 500 mm was carried out using ABAQUS/CAE software.

2.1 Geometry

The dimensions and reinforcement details of the beam, as shown in Figure 1, were meticulously developed in accordance with an approved design supported by Eurocode 2 EN 1992-1-1:2004. Figure 2 shows the finite element analysis model of RC beam.

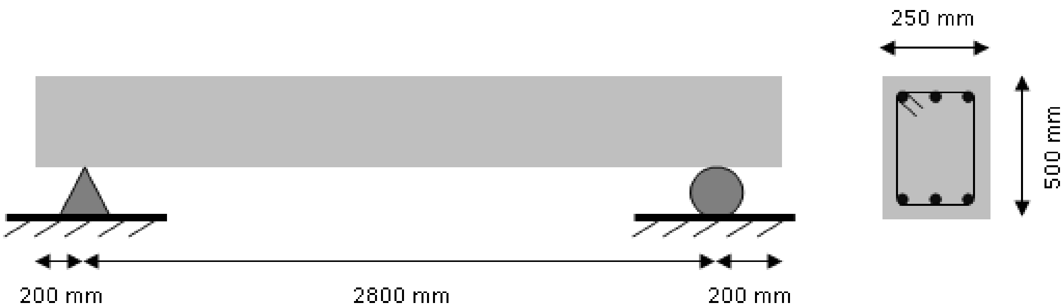

Figure 1: Simply Supported (pin and roller) rectangular RC Beam.

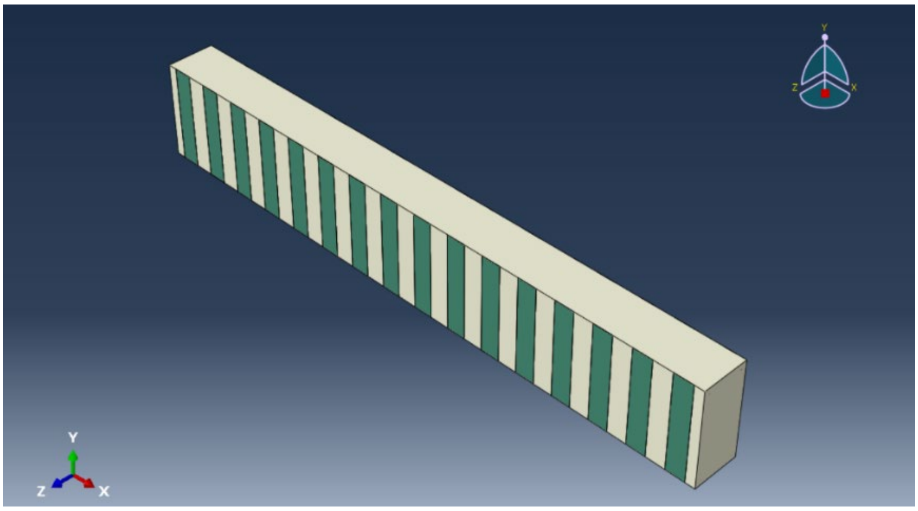

Figure 2: Finite Element Analysis model of RC beam.

2.2 Material

The compressive strength (Fc) of the concrete is specified at 30 MPa, indicating its ability to withstand significant compressive loads. In terms of tensile strength (Ft), the concrete exhibits a value of 2.1 MPa, which is typical for plain concrete without reinforcement. The modulus of elasticity (Ec) of concrete is specified as 25 GPa, indicating its ability to deform elastically under loading and return to its original shape upon unloading. Poisson's ratio (ν) for the material is 0.3, indicating the ratio of lateral strain to longitudinal strain when subjected to axial loading. The density (ρ) of the concrete is 2400 kg/m^3, influencing its weight and mass per unit volume. The tabulated data specify the concrete properties in Table 1. For the yield criterion, ABAQUS uses the function with variables proposed by [8] for the concrete damage plasticity model, where σ_{bo}/σ_{co} represents the initial biaxial compressive yield stress divided by the initial uniaxial compressive yield stress, using the default value in ABAQUS. Kc represents the relative strength of concrete when subjected to equal biaxial compression compared to triaxial compression. Deviatoric plane yield surfaces, which are commonly encountered, can be expressed using varying values of Kc. However, in all FEM simulations, a constant value of 0.667 is used for Kc.

The conventional eccentricity for flow potential is assumed to be 0.1. The magnitude of the dilation angle y is evaluated at various levels of confining pressure, taken as 38°. In the ABAQUS documentation, the viscosity parameter is initially set to 0.0005, as shown in Table 2. Steel reinforcement exhibits a yield strength (Fy) of 420 MPa, indicating the stress level at which it begins to deform plastically. Its modulus of elasticity (Es) is 200 GPa, which defines its stiffness under applied stress. The Poisson's ratio (ν) for steel is 0.3, describing its response to strain in different directions. Additionally, the characteristic strength of steel, denoted fyk, is specified at 500 N/mm^2, indicating the level of strength for both the main reinforcement (12 mm in diameter) and the link reinforcement (8 mm in diameter) used in concrete structures. Table 3 indicates the specified data of steel reinforcement properties.

CFRP is characterized by its thinness, with a thickness of 0.11 mm, making it suitable for applications requiring lightweight reinforcement. It possesses a high modulus of elasticity (Ef) of 230 GPa, indicating its stiffness under applied stress, which is significantly higher than that of steel. The material's tensile strength (Ft) is 3600 MPa, highlighting its exceptional resistance to pulling forces. The density (ρ) of CFRP is 2 g/cm^3, contributing to its lightweight nature, which is advantageous for reducing overall structural weight. Tabulated data for CFRP properties are presented in Table 4.

Table 1: Concrete Properties (Material Design Properties according to EN1992-1-1).

Concrete Properties				
Compressive Strength (Fc)	**Tensile Strength (Ft)**	**Modulus Of Elasticity (Ec)**	**Poisson's Ratio (ν)**	**Density, ρ**
30 MPa	1.2 MPa	31 GPa	0.3	2400 kg/m^3

Table 2: Concrete Damaged Plasticity of Concrete C30 (Numerical Simulation Analysis of Collapse Process of Isolated Structure in Strong Earthquakes, 2018).

Dilation Angle	**Flow Potential Eccentricity**	**Ratio**	**Kc**	**Viscosity Parameter**
38°	0.1000	1.1600	0.66667	0.0005

Table 3: Steel Reinforcement Properties (ASTM A706/A706M-22a-Standard Specification for Deformed and Plain Low-Alloy Steel Bars for Concrete Reinforcement).

Steel Reinforcement Properties				
Yield Strength (Fy)	**Modulus Of Elasticity (Ec)**	**Poisson's Ratio (ν)**	**Characteristic Strength of Steel (Fyk)**	**Characteristic Strength of Link (Fyk)**
420 MPa	200 GPa	0.3	500 N/mm^2	500 N/mm^2

Table 4: Summary Of CFRP Reinforcement Properties (Abbood et al., 2021).

CFRP Properties			
Thickness (mm)	**Tensile Strength (Ft)**	**Modulus Of Elasticity (Ec)**	**Density (ρ)**
0.11	3600 MPa	230 GPa	2 g/cm^3

2.3 Modelling

The analysis focuses on the U-wrapped method of CFRP application, recognized for its efficacy in enhancing shear capacity by confining critical regions of the beam. Figure 3 shows that 90°, 30°, 35°, 40°, 45°, 50°, 55°, and 60° were selected to investigate their influence on shear strength, displacement, compressive strength, and tensile strength. Each one-ply CFRP strip, having a 100 mm width, was applied to maintain consistent material parameters across all eight samples.

The interaction between the CFRP composites and the concrete surface was modelled using shell-to-solid and embedded-region constraints that allow relative movement (slip), providing a more realistic representation of bond behaviour. Amaireh, L.K. and Al-Tamimi, A. validated that in real life, epoxy or resin materials are used to ensure good adhesion between CFRP sheets and concrete [9]. The ABAQUS software allows simulating this either by defining the epoxy as an individual material and assembling it into the model between the concrete and CFRP sheets, or by defining the CFRP composite and then specifying the type of constraint for the beam concrete. Three types of constraints are available in ABAQUS to address this issue. First, the tie constraint connects two separate surfaces so that there is no relative motion between them. Second, a shell-to-solid coupling constraint that allows for coupling the motion of a shell edge to the motion of an adjacent solid face, and the last one is an embedded region constraint that allows for embedding a region of the model within a host region of the model or within the whole model.

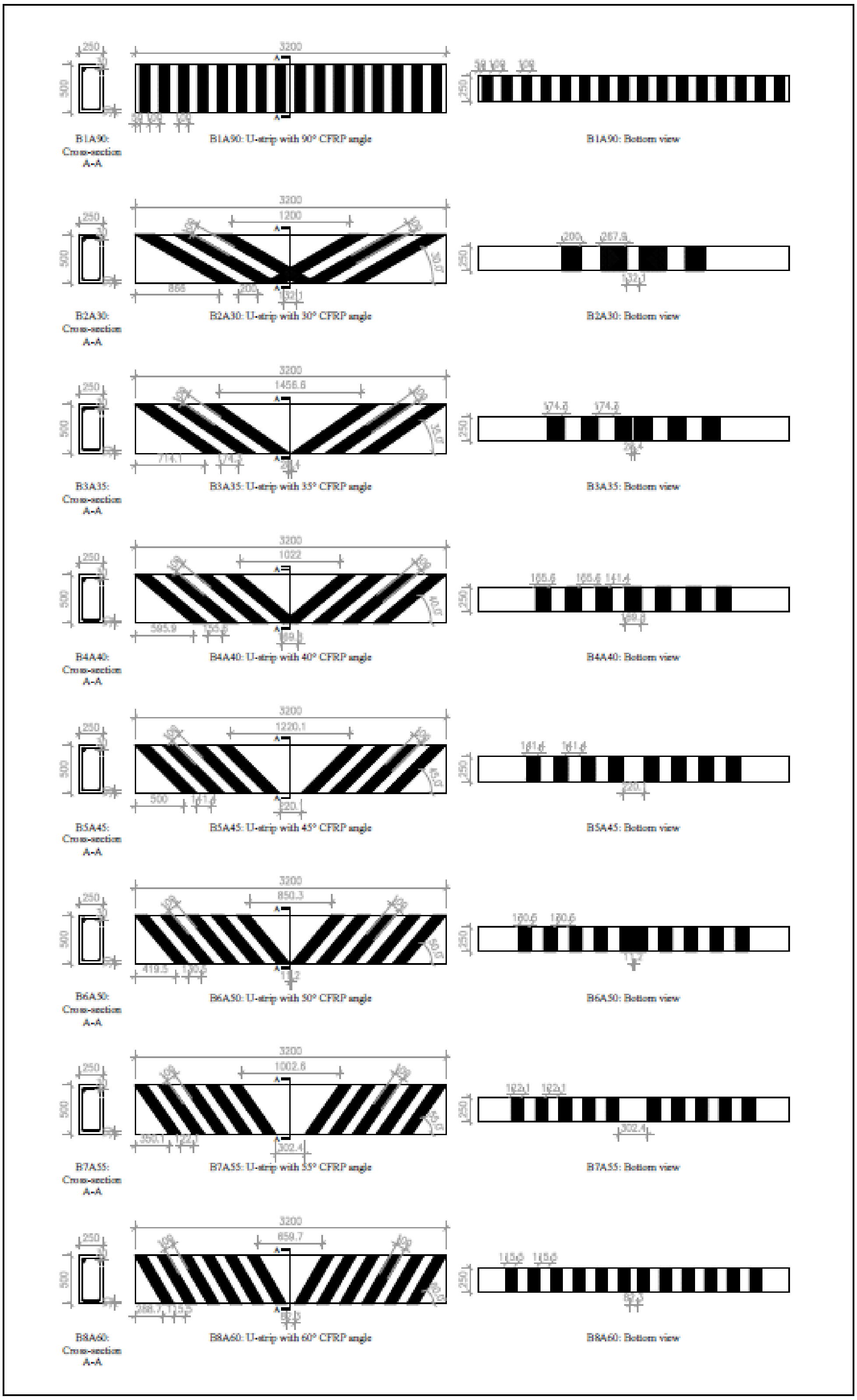

Figure 3: The RC beam model with U-wrapped 90°, 30°, 35°, 40°, 45°, 50°, 55° and 60° CFRP angle.

According to Wang et al. [10], the finite element modelling of concrete is performed using eight-node linear brick elements (C3D8R), effectively capturing its three-dimensional behaviour while optimizing computational efficiency. The reinforcement cage in Figure 4, consisting of longitudinal bars and stirrups, is represented by two-node truss elements (T3D2) and embedded within the concrete matrix using the embedded element constraint method to ensure a perfect bond between the steel and concrete. The bidirectional CFRP materials, including bottom sheets and U-hoops, are modelled using four-node linear reduced-integration shell elements (S4R) in Figure 5, which primarily capture in-plane stiffness, excluding bending stiffness. To mitigate stress concentrations at loading surfaces and supports, analytical rigid components (C3D8R units) are used for both supports and loading components, thereby increasing contact area and stiffness. The final finite element model consisted of approximately 48,000 C3D8R solid elements for the concrete beam, 2,400 T3D2 truss elements for the steel reinforcement, and 1,600 S4R shell elements for the CFRP sheets, resulting in a total of approximately 56,000 nodes.

A mesh sensitivity analysis was conducted to ensure numerical accuracy and mesh-independent results. Three different mesh densities were examined for the concrete domain using 8-node linear brick elements (C3D8R): coarse, medium, and fine. The convergence criterion was based on the displacement response at selected monitoring nodes (Node 9, Node 11, Node 115, and Node 116), located within the shear-critical region of the beam. The results showed that further mesh refinement beyond the medium mesh yielded less than 3% variation in the maximum displacement and stress responses, indicating numerical convergence. Therefore, the medium mesh configuration was adopted in all simulations to achieve a balance between computational efficiency and solution accuracy.

The interaction between the CFRP system and the concrete matrix is modelled using a cohesive surface with the traction-separation approach, following a bi-linear bond-slip law to represent the local CFRP-to-concrete interface behaviour. A displacement nodal point is applied as shown in Figure 6, with displacement convergence criteria set at Node 9 (nodal point in the first row), Node 11(nodal point in the second row), Node 115 (nodal point in the third row) and Node 116 (nodal point in the fourth row) to ensure numerical accuracy. The boundary conditions replicate a four-point bending test with roller and hinged supports.

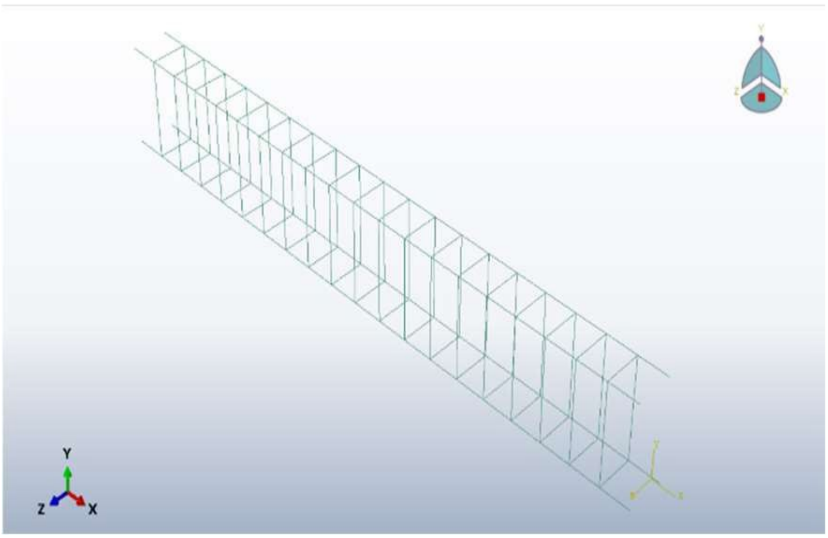

Figure 4: The T3D2 reinforcement model.

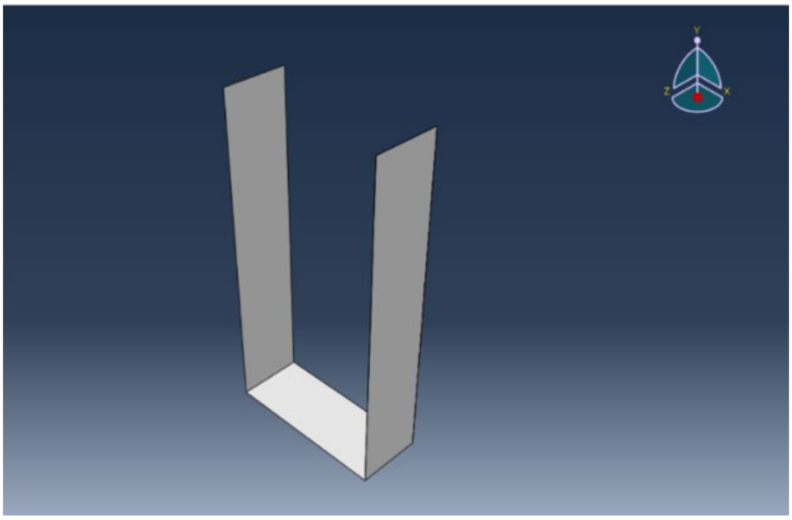

Figure 5: The S4R CFRP model.

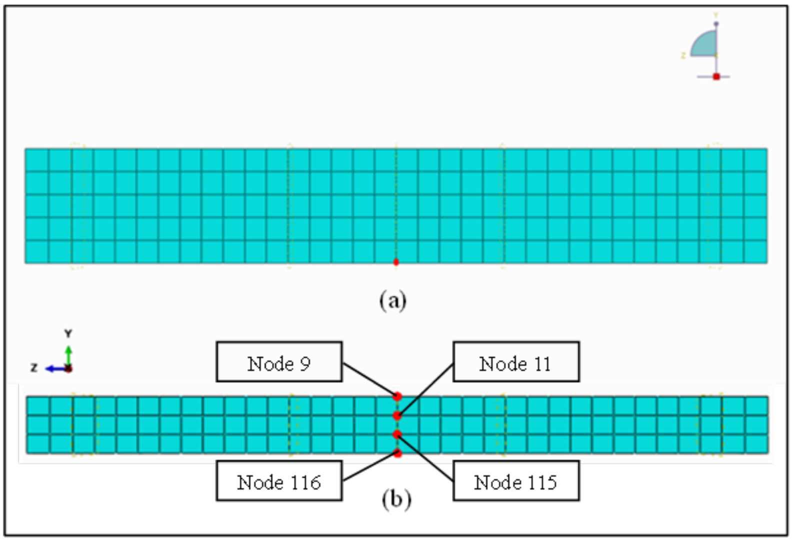

Figure 6: (a) Front view of the FEA model of RC beam, (b) Bottom view of the FEA model.

3. RESULTS AND DISCUSSION

3.1 Displacement

The shear performance of reinforced concrete (RC) beams retrofitted with carbon fibre reinforced polymer (CFRP) is analysed using non-linear finite element analysis (FEA). Using Abaqus software, the research enables precise modelling of complex geometries, material behaviours, and boundary conditions to simulate the intricate interactions between CFRP strips and RC beams under applied loads, as shown in Figure 7. The numerical four-point bending test, as shown in Figure 7 according to ASTM International (2017), is employed to enable an in-depth assessment of stress distribution, strain localization, and failure patterns.

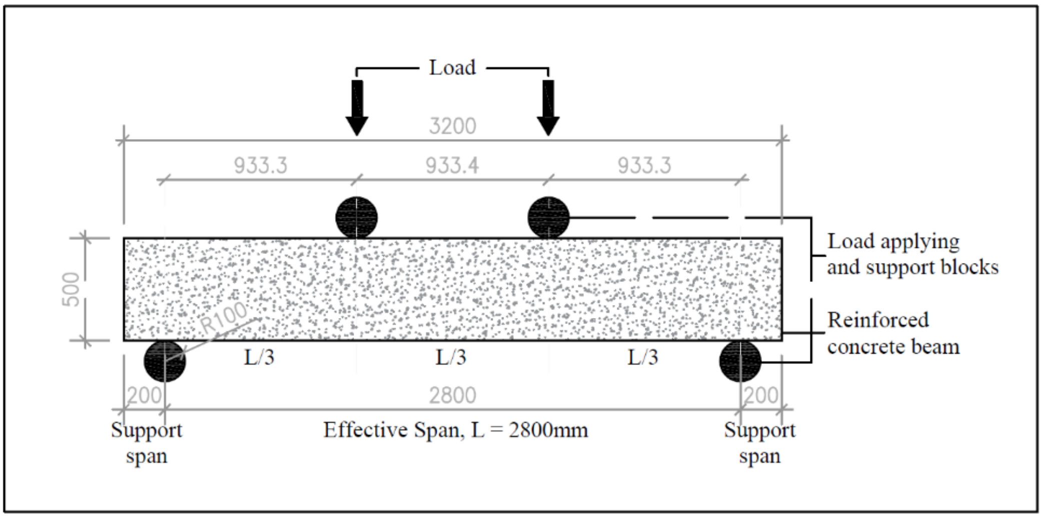

Figure 7: The numerical four-point bending test of the RC beam model.

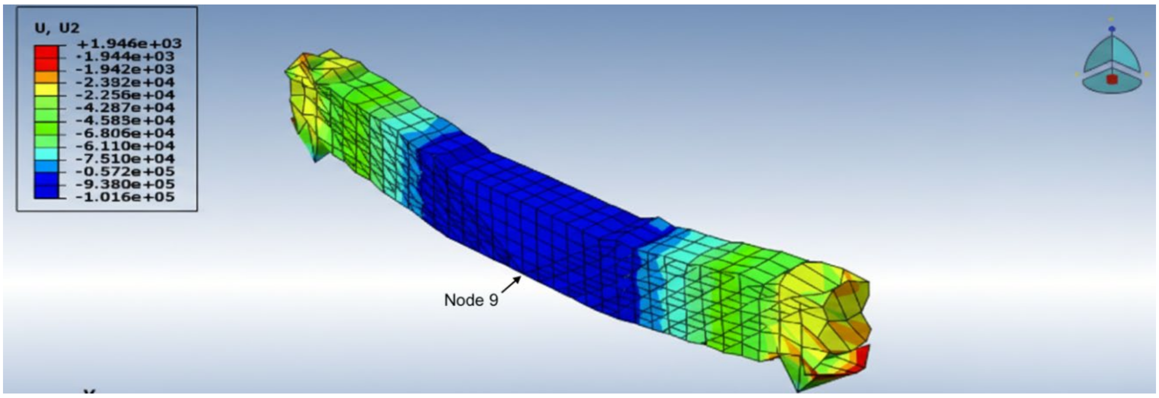

(a)

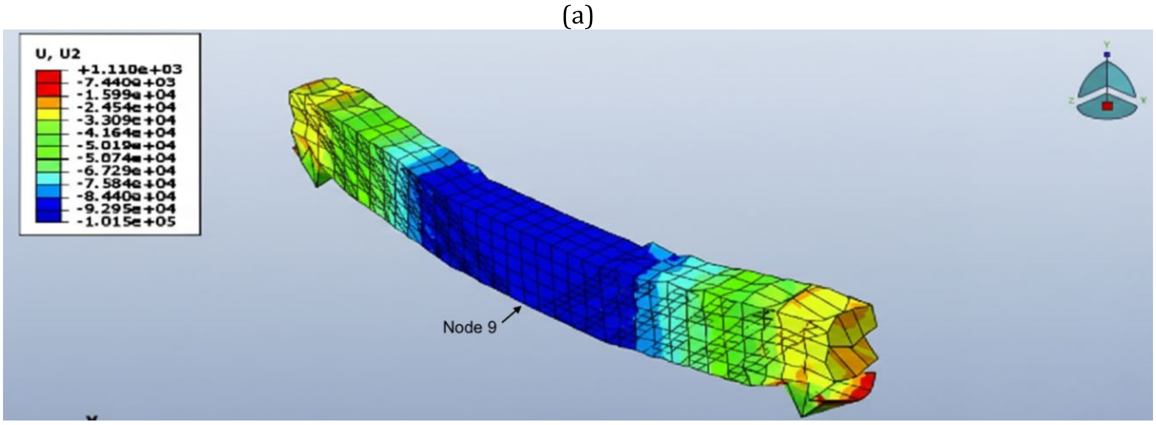

(b)

Figure 8: The displacement of the RC beam with CFRP wrapping angle (a) 45° and (b) 50°.

For lower wrapping angles, such as 30° or 35°, as shown in Figure 8, the average displacement values tend to be higher, indicating reduced stiffness and a greater tendency for deformation. This suggests that the fibres are not optimally aligned to resist the applied shear forces, leading to increased displacement. Conversely, as the wrapping angle increases, the average displacement values show a notable reduction. Wrapping angles around 45° to 50° exhibit the lowest displacement values over time, with the critical location of the result lying on Node 9, as shown in Figure 8. It suggests that these configurations maximize the beam's shear resistance and structural stiffness. Higher wrapping angles, such as 55° or 60°, may also reduce displacement but tend to show diminishing returns. Beyond a certain angle, the alignment of the fibres becomes less effective in resisting shear forces, leading to slightly increased displacement values compared to the optimal range. Based on this analysis, 40° wrapping angle emerges as the optimal configuration for minimizing displacement. This angle effectively balances fibre alignment with the direction of applied shear forces, enhancing the beam's resistance to deformation and improving overall structural performance.

In a typical RC beam, shear cracks usually start to open up at a 45° angle. When we apply the CFRP at 45° to 50°, we are basically placing the fibers almost perfectly perpendicular to those cracks. This creates a strong "bridging" effect; the CFRP strips act like stitches that hold the cracks together. Because the cracks can't open as easily, the beam stays stiffer for a longer time, which explains why the vertical displacement is the lowest at this specific angle. In contrast, when the angle is too low (30°) or too steep (60°), the fibers aren't aligned well enough to catch those diagonal forces. The beam ends up being less rigid, leading to the higher displacement values we saw in the earlier angles. This finding aligns with established theories like the Modified Compression Field Theory (MCFT), which highlights how important fiber orientation is in resisting shear-induced deformation [11,12]. This conclusion highlights the importance of selecting the appropriate CFRP wrapping angle to achieve optimal structural behaviour in RC beam strengthening applications.

3.2 Compressive Stress

The provided data in Figure 9 highlights the compressive stress distribution across four nodes of a reinforced concrete (RC) beam retrofitted with carbon fibre reinforced polymer (CFRP). Based on the analysis of average compressive stress values for the various CFRP wrapping angles shown in Figure 9, several conclusions were drawn regarding the optimal angle for maximizing the compressive strength of reinforced concrete (RC) beams. Each CFRP wrapping angle, ranging from 30° to 60°, was evaluated in terms of its ability to enhance the compressive strength of the concrete, as indicated by the average compressive stress values recorded at 1.0 seconds. The 35° CFRP wrapping angle is the most effective for enhancing compressive strength. At 1.0 second, the average compressive stress reaches 45.473 MPa, the highest among all the angles tested. This indicates that the 35° angle provides the best balance between the lateral confinement of the concrete and its axial strength. The angle appears to be optimal for improving the load-bearing capacity of the concrete, making it the preferred choice for retrofitting RC beams to resist higher axial loads.

In comparison, the 30° CFRP wrapping angle also demonstrates a strong performance, with an average compressive stress of 26.06 MPa at 1.0 second. While this value is relatively high, it is still outperformed by the 35° angle, suggesting that the latter provides slightly better confinement and thus greater strength enhancement. On the other hand, the 40° CFRP wrapping angle results in a lower average compressive stress of 21.138 MPa at 1.0 seconds, indicating that it is less effective in enhancing the compressive strength compared to the 30° and 35° angles.

The 45° CFRP wrapping angle shows moderate performance, with an average compressive stress of 35.634 MPa at 1.0 second. While it provides a noticeable improvement over the 40° angle, it still falls short of the 35° angle in terms of strength enhancement. Similarly, the 50° CFRP wrapping angle results in an average compressive stress of 33.954 MPa at 1.0 second, which is similar to the 45° angle, further suggesting that angles greater than 35° do not significantly improve compressive strength. The 55° and 60° CFRP wrapping angles produce the lowest average compressive stresses at 1.0 second, with values of 16.486 MPa and 19.200 MPa, respectively. These results indicate that higher angles are less effective at enhancing compressive strength, likely due to less efficient lateral confinement and greater difficulty in optimizing the CFRP fibres for maximum load transfer. In conclusion, the 35° CFRP wrapping angle is identified as the optimal angle for enhancing the compressive strength of RC beams, providing the highest average compressive stress at 1.0 second. This angle offers the best performance in improving the axial load resistance of concrete beams, making it the preferred choice for retrofit applications.

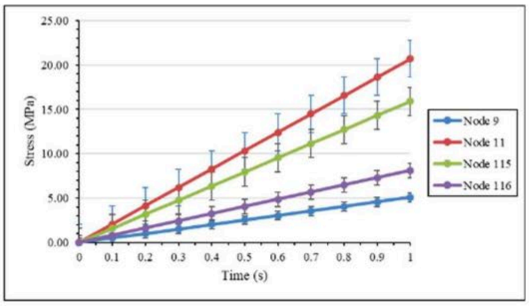

(*a*) 90°

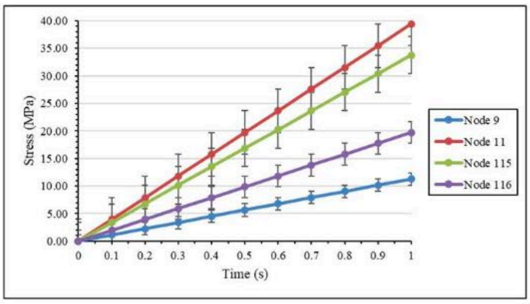

(b) 30°

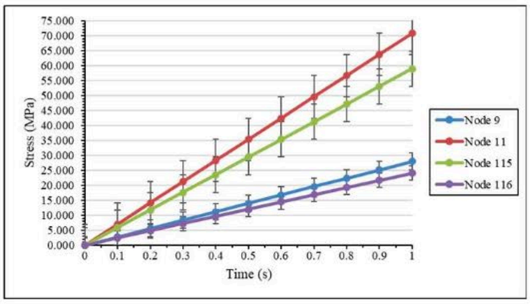

(c) 35°

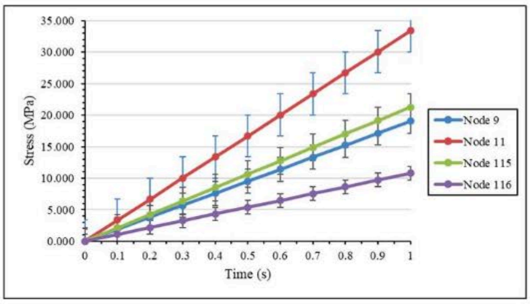

(d) 40°

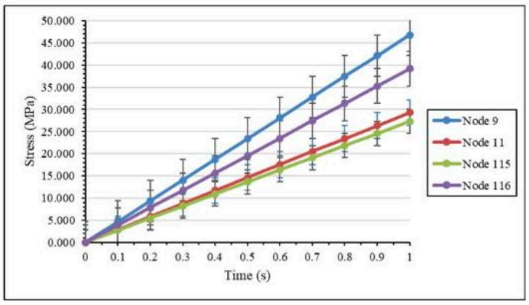

(e) 45°

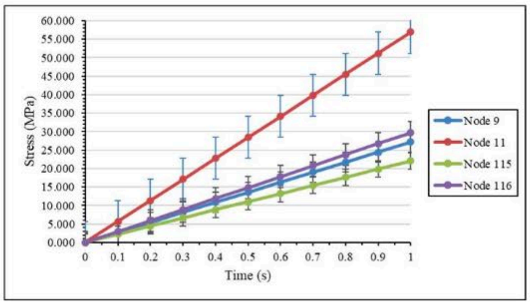

(f) 50°

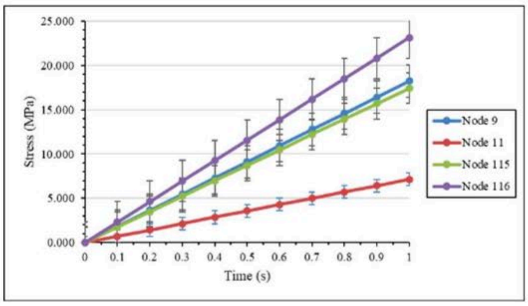

(g) 55°

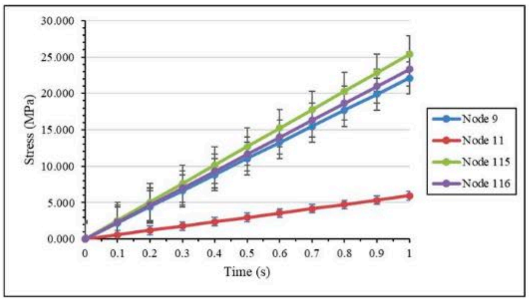

(h) 60°

Figure 9: The stress-time graph of the RC beam with CFRP wrapping angle.

Looking at the data, the peak compressive stress of 45.473 MPa at a 35° angle is a standout result. This really highlights how effective the confinement effect is when the angle is just right. To put it simply, when concrete is under heavy pressure, it naturally wants to push outwards. This is known as the Poisson effect. By wrapping the beam at a 35° angle, the CFRP acts like a high-strength hoop that tightly holds the concrete together.

This effect is crucial because it forces the concrete into a state of triaxial compression. Instead of just being squashed from the top, the concrete is also supported from the sides. This prevents internal microcracks from spreading too quickly, effectively delaying the concrete from crushing. Compared to steeper angles, the 35° orientation seems to strike the best balance in distributing these lateral forces, significantly boosting the beam's overall load-carrying capacity and ductility before it fails [13,14].

3.3 Tensile Stress

The analysis of the average tensile stress values across varying CFRP wrapping angles (from 30° to 60°) reveals a clear trend: as the angle increases, the tensile stress capacity of the reinforced concrete (RC) beams improves significantly. This trend reflects the interaction between the concrete's inherent behaviour under tensile loading and the strengthening effects of the CFRP material. In terms of concrete behaviour, concrete is generally strong in compression but weak in tension. Under bending or loading conditions, the tensile stresses tend to accumulate in the lower portion of the beam, where cracks often initiate. The application of CFRP wrapping, particularly at higher angles, enhances the beam's ability to resist these tensile forces by providing external confinement and increasing the strain capacity of the concrete. As the CFRP wrapping angle increases, the material's fibres are oriented in a way that better aligns with the tensile stresses in the beam, allowing for more efficient load transfer and stress distribution. This is why higher angles, such as 55° and 60°, show a dramatic increase in tensile stress values, as the CFRP fibres are better oriented to resist the tensile forces acting on the beam.

From a physics perspective, the behaviour of the RC beam with CFRP reinforcement can be explained by the principles of material mechanics. The CFRP fibres, which are highly tensile, significantly enhance the beam's tensile strength. When wrapped at higher angles, the CFRP fibres distribute the load more effectively across the beam, reducing the likelihood of localized failure and crack propagation. The increase in tensile stress at higher wrapping angles results from the composite action between the concrete and CFRP, with the CFRP acting as external reinforcement that resists forces that would otherwise cause the concrete to fail. As the wrapping angle increases, the effectiveness of this reinforcement improves, leading to higher tensile stress values and a more robust structural performance.

The results show that 60° CFRP wrapping provides the highest average tensile stress, indicating that this angle offers the most efficient reinforcement in terms of concrete behaviour and physics principles. At this angle, the CFRP material is optimally aligned to resist tensile forces in the beam, resulting to the greatest increase in tensile capacity. This behaviour is a direct result of the synergy between the concrete's weak tensile strength and the CFRP's high tensile strength, with the latter providing an external support system that enhances the overall performance of the RC beam. In conclusion, 60° CFRP wrapping emerges as the optimal angle for maximizing the tensile strength of RC beams, combining the principles of concrete behaviour and material mechanics.

Tensile stress, a measure of the beam's resistance to elongation, reached its maximum value of 31.23 MPa at the 60° wrapping angle, as shown in Figure 10. This configuration aligns the CFRP fibres with the principal tensile stress trajectories, improving the beam's resistance to cracking and tensile failure. The significant increase in tensile stress capacity at the 60° wrapping angle (31.23 MPa) is particularly interesting as it suggests the CFRP is contributing to the beam's flexural resistance. At this steeper angle, the fibers align more closely with the principal tensile stress trajectories at the bottom of the beam. Zhang and Wei [15] observed that when fiber orientation approaches the longitudinal axis of the beam, the CFRP begins to share a larger portion of the tensile load with the internal steel reinforcement.

This behavior is further supported by the work of Li et al. [16], who demonstrated that the interaction between fiber orientation and principal stress paths determines the ultimate tensile capacity of the composite system. Using an inclined wrap results in more efficient stress transfer across the tension zone. As highlighted in numerical simulations by Hassan and El-Zohairy [17], inclined strips are highly effective at bridging the gap between localized cracks, preventing them from merging into a major failure plane. Ultimately, as supported by Nouri and Amrouche [18], the 60° model reached the highest tensile values because the fibers were optimally positioned to resist the longitudinal pulling forces that dominate during the final stages of loading.

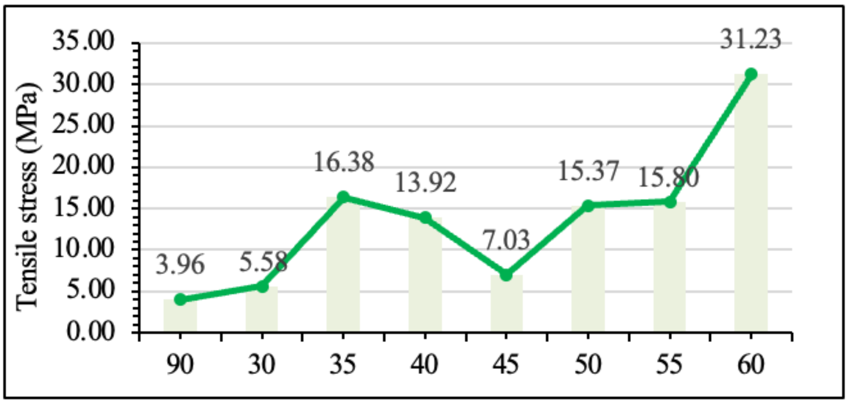

Figure 10: The stress-time graph of RC beam with $90^{\circ}, 30^{\circ}, 35^{\circ}, 40^{\circ}, 45^{\circ}, 50^{\circ}, 55^{\circ}$ *and* 60° CFRP wrapping angle.

3.4 Limitation of study

While the FEA results provide valuable insights into the influence of CFRP wrapping angles, it is important to acknowledge certain limitations inherent in this study. Firstly, the numerical model assumes a perfect bond between the CFRP strips and the concrete surface. In real-world applications, failure often occurs due to debonding or delamination of the CFRP before the material reaches its full tensile strength [19]. Because this simulation did not fully account for the complex adhesive-concrete interface properties, the predicted stress values might be slightly more optimistic than experimental results. Secondly, this research focused primarily on the short-term static loading behavior of the RC beams. In practice, these structures are often subjected to long-term environmental factors, such as temperature fluctuations and humidity, which can degrade the epoxy resins used in CFRP systems [20]. Lastly, the study was limited to a specific beam geometry and concrete grade. While the trends observed are scientifically grounded, the optimal angles found, which are 35°, 40°, and 60°, might vary slightly depending on the shear-span-to-depth ratio (a/d) or the presence of internal stirrups, which were not the primary focus of this analysis.

4. CONCLUSION

This study investigated the influence of Carbon Fiber Reinforced Polymer (CFRP) orientations on the shear strengthening of reinforced concrete (RC) beams using Finite Element Analysis (FEA). Among the tested configurations, the 40° wrapping angle (B4A40) proved the most effective, minimizing displacement while providing balanced compressive and tensile stress resistance. This alignment optimized the interaction between CFRP fibers and concrete, effectively bridging cracks and redistributing shear forces. Wrapping angles of 45° and 50° also performed well, aligning fibers with principal shear stress trajectories. Lower angles, such as 30° and 35°, showed reduced stiffness, while higher angles, like 55° and 60°, exhibited diminishing returns.

The study achieved its objectives by modelling and analysing RC beams with various CFRP orientations, identifying 40° as the optimal angle for shear strengthening. These findings offer practical solutions for retrofitting RC structures to enhance durability and performance. Applications include strengthening load-bearing elements in residential and industrial buildings to withstand seismic forces and dynamic loads. Future research should focus on experimental validation of FEA results, exploring variables such as CFRP thickness, hybrid orientations, and dynamic loading conditions. Economic feasibility studies and collaboration with industry stakeholders can ensure practical implementation, advancing the use of CFRP for safer, more resilient, and sustainable construction practices.

ACKNOWLEDGEMENTS

This research was supported by the Ministry of Higher Education Malaysia (MOHE) through the Fundamental Research Grant Scheme (FRGS/1/2023/TK06/UNIMAP/02/1), which made this research possible.

REFERENCES

[1] Hamakareem, M. I. What is reinforced concrete? Uses, benefits, and advantages. The Constructor (2019).
[2] Unitrade. Beam construction materials in superstructure for buildings. SYARIKAT LOGAM UNITRADE (2023).
[3] Katlav, M., Türk, K., Turğut, P. Flexural performance of V-shaped RC folded plates: The role of plate thickness and fiber hybridization. Construction and Building Materials, vol 400 (2023) pp.132815. https://doi.org/10.1016/j.conbuildmat.2023.132815
[4] Yu, F., Xu, G., Niu, D., Cheng, A., Wu, P., Kong, Z. Experimental study on PVC-CFRP confined concrete columns under low cyclic loading. Construction and Building Materials, vol 177 (2018) pp.287-302. https://doi.org/10.1016/j.conbuildmat.2018.05.111
[5] Jin, L., Zhang, J., Liu, D., Du, X. Meso-scale analysis of shear performance and size effect of CFRP sheets strengthened RC beams. Structures, vol 45 (2022) pp.1630-1645. https://doi.org/10.1016/j.istruc.2022.09.104
[6] Chalioris, C. E., Zapris, A. G., Karayannis, C. G. U-jacketing applications of fiber-reinforced polymers in reinforced concrete T-beams against shear-Tests and design. Fibers, vol 8, issue 2 (2020) pp.13. https://doi.org/10.3390/fib8020013
[7] Mhanna, H. H., Hawileh, R. A., Abdalla, J. A. Shear strengthening of reinforced concrete T-beams using CFRP laminates anchored with bent CFRP splay anchors. Procedia Structural Integrity, vol 28 (2020) pp.811-819. https://doi.org/10.1016/j.prostr.2020.10.095
[8] Uz, M. E., Guner, Y., Avci, E. Strengthening of reinforced concrete beams via CFRP orientation. Buildings, vol 14 (2023) pp.82. https://doi.org/10.3390/buildings14010082
[9] Amaireh, L. K., Al-Tamimi, A. Optimum configuration of CFRP composites for strengthening of reinforced concrete beams considering the contact constraint. Procedia Manufacturing, vol 44 (2020) pp.350-357. https://doi.org/10.1016/j.promfg.2020.02.284
[10] Wang, Y., Zheng, H., Chen, H., Chen, Z., Zhuang, N. Experimental and numerical study on the flexural properties of RC beams with different CFRP-strengthened schemes. Journal of Building Engineering (2024) pp.110734. https://doi.org/10.1016/j.jobe.2024.110734
[11] Khalifa, A., Nanni, A. Rehabilitation of rectangular shear critical reinforced concrete beams with CFRP laminates. Cement and Concrete Composites, vol 24 (2002) pp.309-316.
[12] Islam, M. R., Mansur, M. A., Maalej, M. Shear strengthening of RC deep beams using externally bonded FRP systems. Cement and Concrete Composites, vol 27 (2005) pp.413-420. https://doi.org/10.1016/j.cemconcomp.2004.04.002
[13] Lin, G., Teng, J. G. Advanced stress-strain model for FRP-confined concrete in RC columns. Engineering Structures, vol 210 (2020) pp.110314. https://doi.org/10.1016/j.compositesb.2020.108149
[14] Al-Fakih, A., Wahab, N., Roslan, M. S. Enhancement of compressive strength of reinforced concrete beams using external CFRP wrapping: A numerical study. Structures, vol 58 (2023) pp.1021-1035.

[15] Zhang, Y., Wei, Y. Flexural behavior of RC beams strengthened with CFRP: Effect of fiber orientation and reinforcement ratio. Journal of Building Engineering, vol 43 (2021) pp.102537.
[16] Li, S., Zhao, X., Singh, A. Interaction between CFRP fiber orientation and principal stress paths in reinforced concrete members. Composite Structures, vol 312 (2023) pp.116842.
[17] Hassan, M., El-Zohairy, A. Numerical simulation of the tensile performance of RC beams strengthened with inclined CFRP strips. Structures, vol 48 (2023) pp.1245-1260.
[18] Nouri, M., Amrouche, A. Experimental and numerical investigation on the effect of CFRP wrapping angle on the tensile capacity of RC beams. Engineering Structures, vol 301 (2024) pp.117325.
[19] Smith, S. T., Teng, J. G. FRP-strengthened RC beams. II: Assessment of debonding strength models. Engineering Structures, vol 24 (2002) pp.397-417. https://doi.org/10.1016/S0141-0296(01)00106-7
[20] Xian, G., Guo, R., Li, C., Wang, Y. Effects of environmental adaptation on the long-term performance of CFRP plates: A review. Composite Structures, vol 264 (2021) pp.113717.

Conflict of interest statement: The authors declare no conflict of interest.

Author contributions statement: Conceptualization, Rishitaran Pannir Selvam & N A Hashim; Methodology, Rishitaran Pannir Selvam; Formal Analysis, Rishitaran Pannir Selvam; Resources, N A Hashim; Data Curation, Rishitaran Pannir Selvam & N A Hashim; Writing, Rishitaran Pannir Selvam & N A Hashim; Writing Review & Editing, N A Hashim & H N Yakin; Visualization, Rishitaran Pannir Selvam; Supervision, N A Hashim; Project Administration, N A Hashim; Funding Acquisition, N A Hashim & H N Yakin.

Data Availability Statement: All data generated or analyzed during this study are included in this published article.

APPENDIX

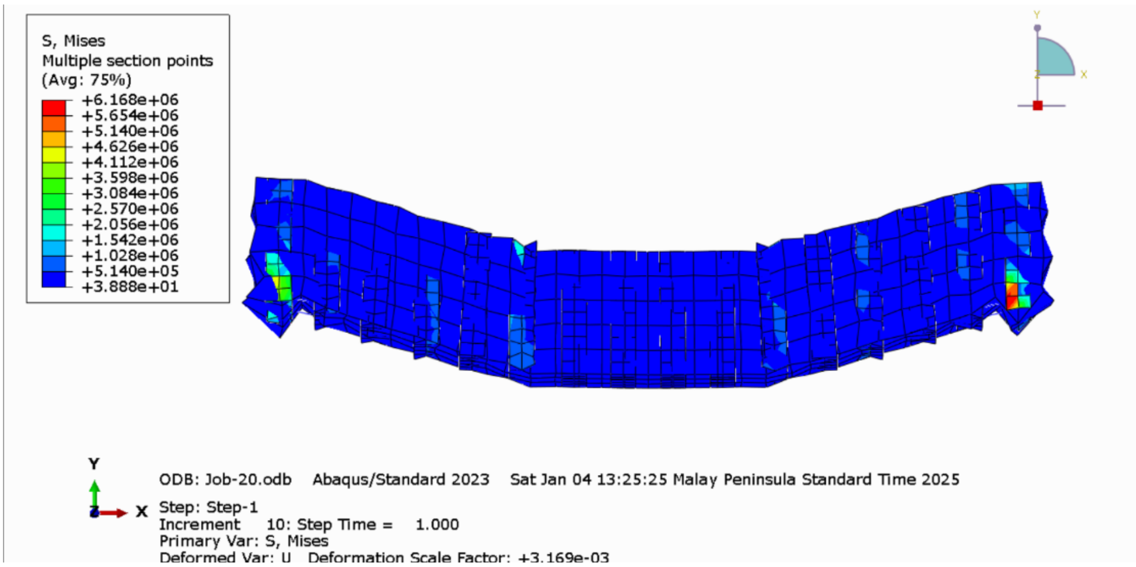
S, Mises
Multiple section points
(Avg: 75%)
+6.168e+06
+5.654e+06
+5.140e+06
+4.626e+06
+4.112e+06
+3.598e+06
+3.084e+06
+2.570e+06
+2.056e+06
+1.542e+06
+1.028e+06
+5.140e+05
+3.888e+01
Y
X
ODB: Job-20.odb Abaqus/Standard 2023 Sat Jan 04 13:25:25 Malay Peninsula Standard Time 2025
Step: Step-1
Increment 10: Step Time = 1.000
Primary Var: S, Mises
Deformed Var: U Deformation Scale Factor: +3.169e-03

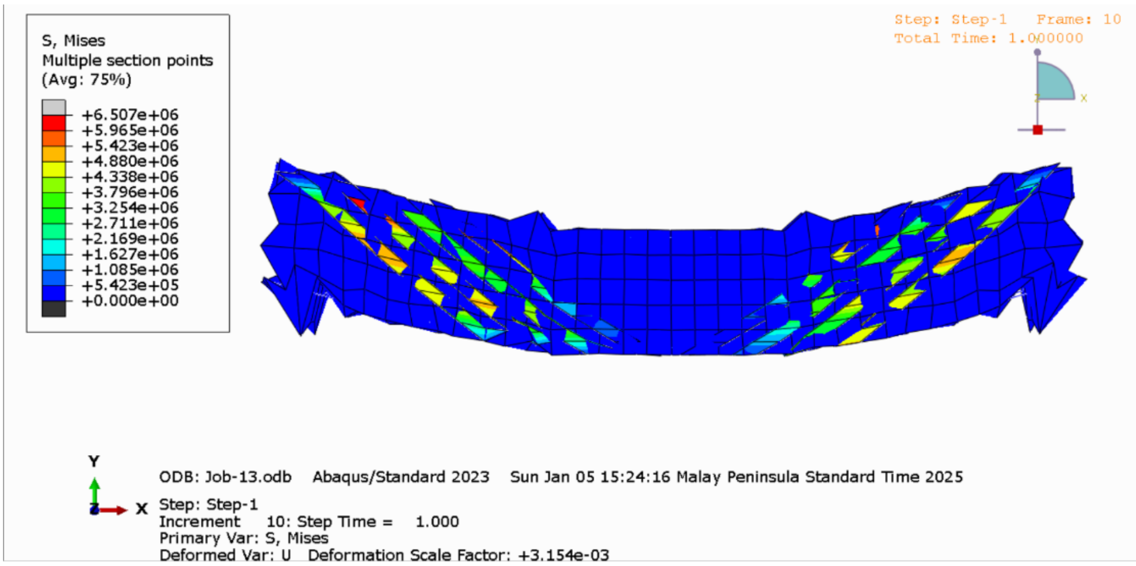
S, Mises
Multiple section points
(Avg: 75%)
+6.507e+06
+5.965e+06
+5.423e+06
+4.880e+06
+4.338e+06
+3.796e+06
+3.254e+06
+2.711e+06
+2.169e+06
+1.627e+06
+1.085e+06
+5.423e+05
+0.000e+00
Step: Step-1 Frame: 10
Total Time: 1.000000
Y
X
ODB: Job-13.odb Abaqus/Standard 2023 Sun Jan 05 15:24:16 Malay Peninsula Standard Time 2025
Step: Step-1
Increment 10: Step Time = 1.000
Primary Var: S, Mises
Deformed Var: U Deformation Scale Factor: +3.154e-03

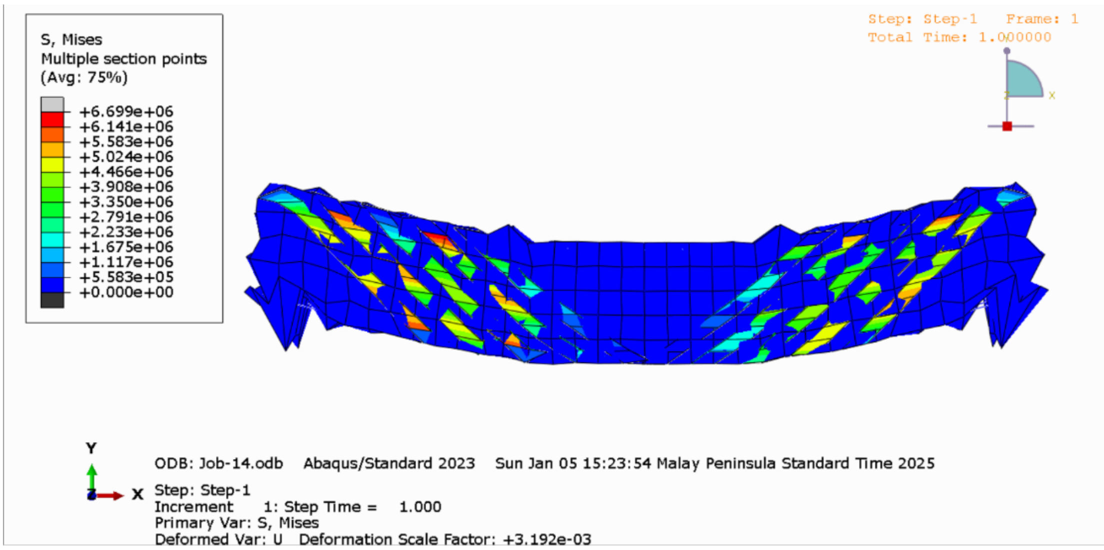
S, Mises
Multiple section points
(Avg: 75%)
+6.699e+06
+6.141e+06
+5.583e+06
+5.024e+06
+4.466e+06
+3.908e+06
+3.350e+06
+2.791e+06
+2.233e+06
+1.675e+06
+1.117e+06
+5.583e+05
+0.000e+00
Step: Step-1 Frame: 1
Total Time: 1.000000
ODB: Job-14.odb Abaqus/Standard 2023 Sun Jan 05 15:23:54 Malay Peninsula Standard Time 2025
Step: Step-1
Increment 1: Step Time = 1.000
Primary Var: S, Mises
Deformed Var: U Deformation Scale Factor: +3.192e-03

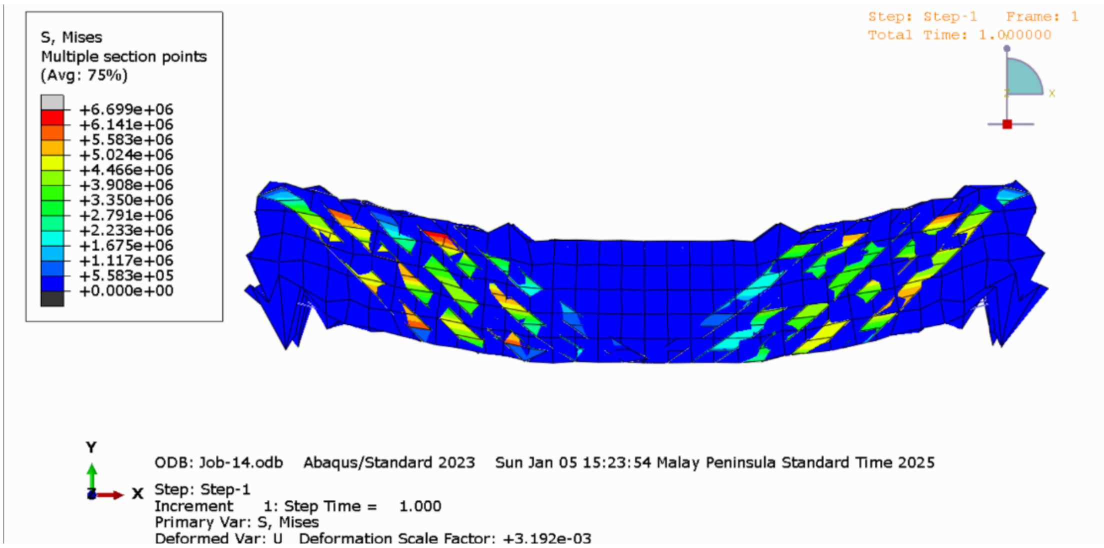
S, Mises
Multiple section points
(Avg: 75%)
+6.699e+06
+6.141e+06
+5.583e+06
+5.024e+06
+4.466e+06
+3.908e+06
+3.350e+06
+2.791e+06
+2.233e+06
+1.675e+06
+1.117e+06
+5.583e+05
+0.000e+00
Step: Step-1 Frame: 1
Total Time: 1.000000
ODB: Job-14.odb Abaqus/Standard 2023 Sun Jan 05 15:23:54 Malay Peninsula Standard Time 2025
Step: Step-1
Increment 1: Step Time = 1.000
Primary Var: S, Mises
Deformed Var: U Deformation Scale Factor: +3.192e-03

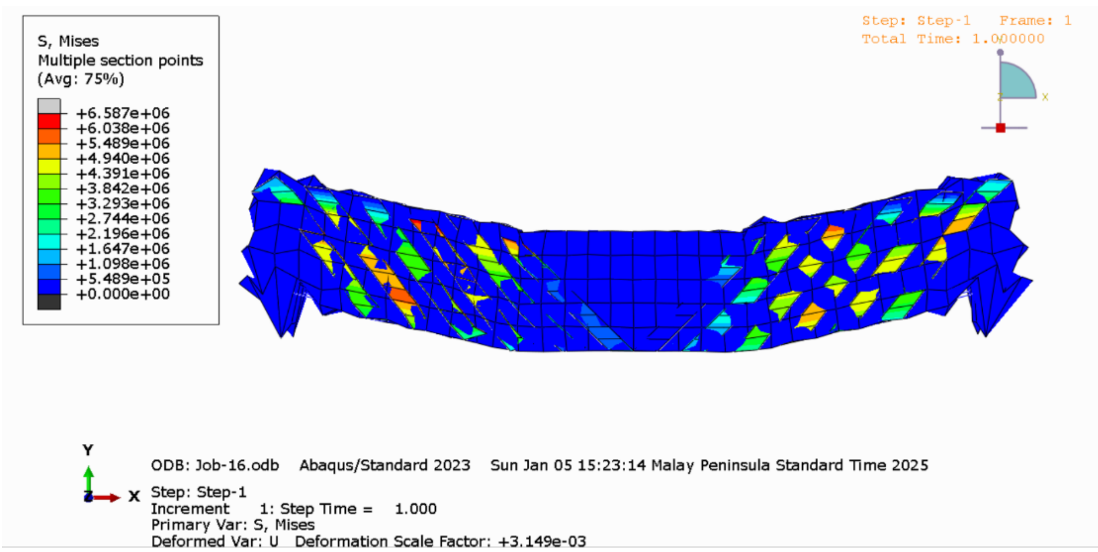
S, Mises
Multiple section points
(Avg: 75%)
+6.587e+06
+6.038e+06
+5.489e+06
+4.940e+06
+4.391e+06
+3.842e+06
+3.293e+06
+2.744e+06
+2.196e+06
+1.647e+06
+1.098e+06
+5.489e+05
+0.000e+00
Step: Step-1 Frame: 1
Total Time: 1.000000
ODB: Job-16.odb Abaqus/Standard 2023 Sun Jan 05 15:23:14 Malay Peninsula Standard Time 2025
Step: Step-1
Increment 1: Step Time = 1.000
Primary Var: S, Mises
Deformed Var: U Deformation Scale Factor: +3.149e-03

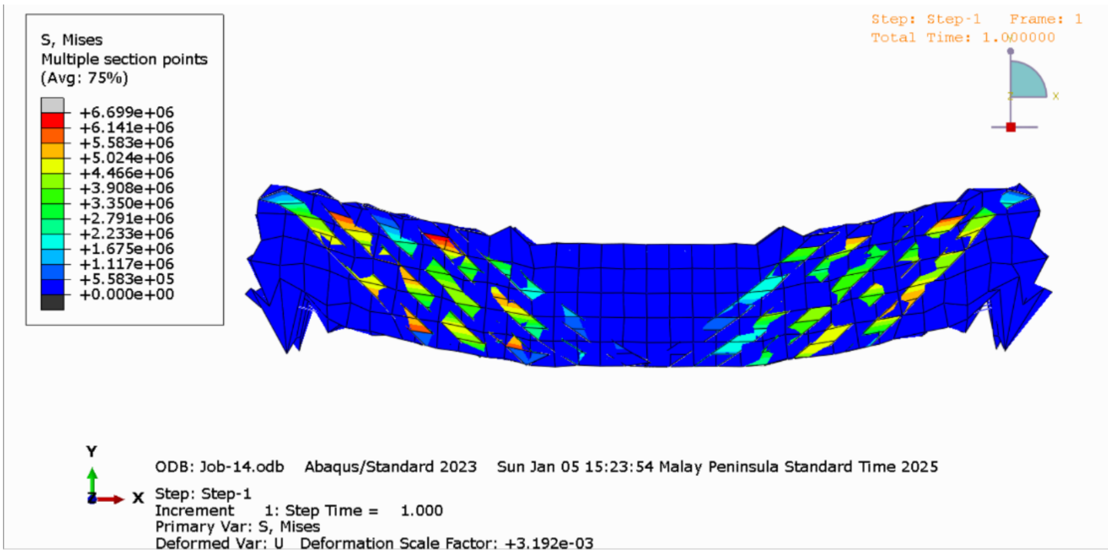
S, Mises
Multiple section points
(Avg: 75%)
+6.699e+06
+6.141e+06
+5.583e+06
+5.024e+06
+4.466e+06
+3.908e+06
+3.350e+06
+2.791e+06
+2.233e+06
+1.675e+06
+1.117e+06
+5.583e+05
+0.000e+00
Step: Step-1 Frame: 1
Total Time: 1.000000
Y
X
ODB: Job-14.odb Abaqus/Standard 2023 Sun Jan 05 15:23:54 Malay Peninsula Standard Time 2025
Step: Step-1
Increment 1: Step Time = 1.000
Primary Var: S, Mises
Deformed Var: U Deformation Scale Factor: +3.192e-03

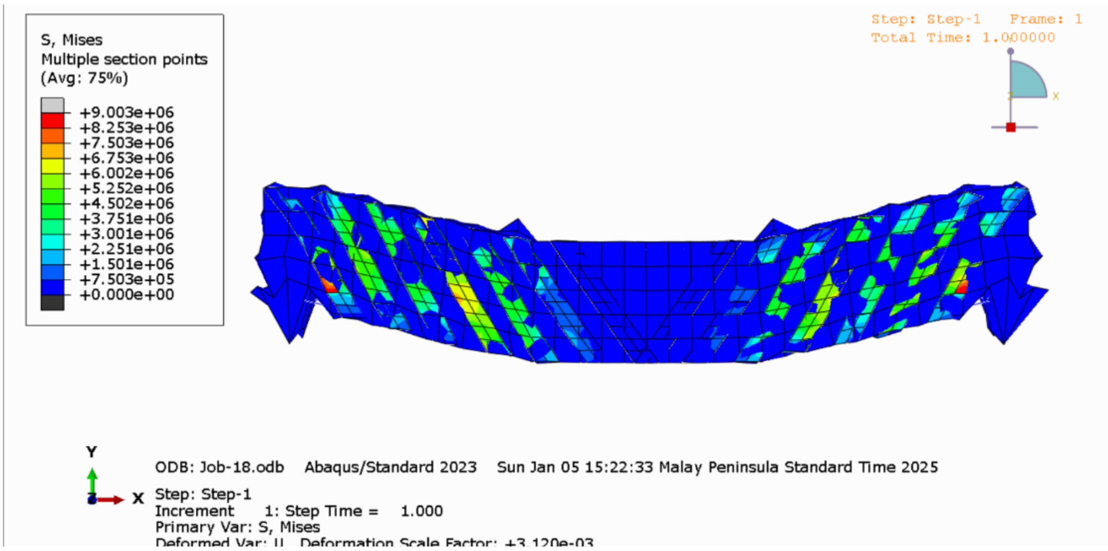
S, Mises
Multiple section points
(Avg: 75%)
+9.003e+06
+8.253e+06
+7.503e+06
+6.753e+06
+6.002e+06
+5.252e+06
+4.502e+06
+3.751e+06
+3.001e+06
+2.251e+06
+1.501e+06
+7.503e+05
+0.000e+00
Step: Step-1 Frame: 1
Total Time: 1.000000
Y
X
ODB: Job-18.odb Abaqus/Standard 2023 Sun Jan 05 15:22:33 Malay Peninsula Standard Time 2025
Step: Step-1
Increment 1: Step Time = 1.000
Primary Var: S, Mises
Deformed Var: U Deformation Scale Factor: +3.120e-03

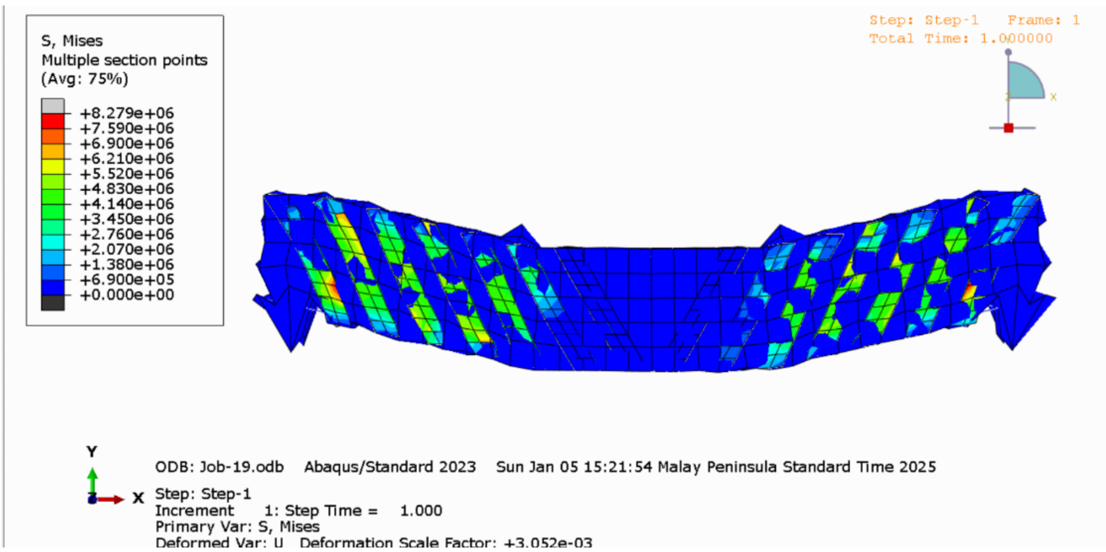
S, Mises
Multiple section points
(Avg: 75%)
+8.279e+06
+7.590e+06
+6.900e+06
+6.210e+06
+5.520e+06
+4.830e+06
+4.140e+06
+3.450e+06
+2.760e+06
+2.070e+06
+1.380e+06
+6.900e+05
+0.000e+00
Step: Step-1 Frame: 1
Total Time: 1.000000
Y
X
ODB: Job-19.odb Abaqus/Standard 2023 Sun Jan 05 15:21:54 Malay Peninsula Standard Time 2025
Step: Step-1
Increment 1: Step Time = 1.000
Primary Var: S, Mises
Deformed Var: U Deformation Scale Factor: +3.052e-03